Radiological Physics and Technology (2019) 12:417–425
https://doi.org/10.1007/s12194-019-00531-9

A mask method to assess the uniformity of fat suppression in phantom studies

Yasuo Takatsu[1,2] · Masafumi Nakamura[3] · Kenichiro Yamamura[4] · Satoshi Sawa[5] · Masaki Asahara[1] · Michitaka Honda[1] · Tosiaki Miyati[2]

Received: 3 May 2019 / Revised: 7 August 2019 / Accepted: 7 August 2019 / Published online: 17 August 2019

Abstract
Fat suppression is a technique used to suppress the signals from adipose tissues, during clinical evaluation of the tissues near the fat–tissue boundary. However, in cases where the scan area has a complicated shape, the effect of fat suppression may demonstrate poor uniformity, resulting in diagnosis-related difficulties. To improve the uniformity of fat suppression, phantom studies are more suitable than volunteer studies. In this study, we evaluated the reliability of the region of interest (ROI) dependency using an unevenness phantom, to develop a method to assess the uniformity of fat suppression while using whole magnetic resonance imaging by masking the surrounding phantom. We modulated different ROI sizes, which were eroded from 100% to approximately 50%, and observed that the normalized absolute average deviation and error increased with decreased ROI. Using our method, more objective, concrete, and accurate data could be obtained by including the whole-body phantom (whole poor uniformity area).

Keywords Magnetic resonance imaging · Fat suppression · Uniformity · Normalized absolute average deviation · Mask method

1 Introduction

In magnetic resonance imaging (MRI), fat suppression is used to suppress signals from adipose tissues, during clinical evaluation of tissues near a fat–tissue boundary. Typically, a frequency-selective fat suppression method can be used to nullify fat signals in an image, to observe contrast enhancement using a contrast medium [1–3].

However, if the scan area has a complicated shape, such as the cervical region, it is possible that the effect of fat suppression may demonstrate poor uniformity [4], resulting in diagnosis-related difficulties. Distinguishing between high signal intensity from inadequate fat suppression and that due to contrast enhancement could be particularly difficult.

Several methods to improve uniformity of fat suppression have previously been reported, such as volume-shimming [5],

✉ Yasuo Takatsu
pcblue2@yahoo.co.jp

Masafumi Nakamura
nakamura-xx@leto.eonet.ne.jp

Kenichiro Yamamura
rad047@osaka-med.ac.jp

Satoshi Sawa
sa.sawa@hotmail.co.jp

Masaki Asahara
asahara@kgw.bunri-u.ac.jp

Michitaka Honda
hondam@kgw.bunri-u.ac.jp

Tosiaki Miyati
ramiyati@mhs.mp.kanazawa-u.ac.jp

[1] Department of Radiological Technology, Faculty of Health and Welfare, Tokushima Bunri University, 1314-1 Shido, Sanuki, Kagawa 769-2193, Japan

[2] Division of Health Sciences, Graduate School of Medical Sciences, Kanazawa University, 5-11-80 Kodatsuno, Kanazawa 920-0942, Japan

[3] Department of Radiology, Otsu City Hospital, 2-9-9, Motomiya, Otsu, Shiga 520-0804, Japan

[4] Department of Radiology, Osaka Medical College Hospital, 2-7, Daigaku-cho, Takatsuki, Osaka 569-8686, Japan

[5] Department of Diagnostic Radiology, Japanese Red Cross Society Kyoto Daiichi Hospital, 15-749, Honmachi, Higashiyama-ku, Kyoto 605-0981, Japan

use of improvement assistance materials [6], and selection of an optimal fat suppression method [4, 7]. While assessing the sequence parameter or performing a volume-shimming, particularly considering the long scanning time, a phantom study would be considerably more suitable than a volunteer study, excluding the influence of the moving artifacts.

The uniformity of fat suppression can be evaluated via a physical assessment using a phantom [5, 7] and visual assessment [8, 9]; however, the former is significantly more advantageous as it provides an objective quantification.

One of the assessments of the uniformity is peak deviation non-uniformity (PIU) by calculating the maximum (S_{max}) and minimum signals (S_{min}) within a region of interest (ROI). The ROI is set at a minimum 75% area of the phantom image. The PIU is calculated by the following equation [10]:

$$\mathrm{PIU} = 100 \times \left[1 - \frac{(S_{max} - S_{min})}{(S_{max} + S_{min})}\right].$$

Moreover, to reduce the influence of image signal-to-noise ratio (SNR), a normalized absolute average deviation (NAAD) is used to evaluate the uniformity [10]. NAAD is calculated using the following equation:

$$\mathrm{NAAD} = 100 \times \left[1 - \frac{1}{N\bar{Y}} \sum_{i=1}^{N} (|Y_i - \bar{Y}|)\right].$$

Here, Y_i is the individual pixel value within the measurement ROI (MROI), $\bar{Y}$ is the mean of all pixels within the MROI, $|Yi - Y|$ is the absolute deviation for pixel *i,* and N is the total number of the pixels within the MROI [10].

To obtain accurate measurements of the uniformity of fat suppression, the selection of the ROI is critical. Poor uniformity of fat suppression is frequently observed in the peripheral region, away from the center of the image. Therefore, the ROI may not include the areas of poor uniformity in the peripheral regions, while using the conventional ROI (square or circle) (Fig. 1a–c), even if several small ROIs were used. In addition, the ROI was set at a 75% area of the phantom image, and the areas of poor uniformity could not be assessed. Therefore, we set a threshold value to identify the regions demonstrating high signal intensity due to

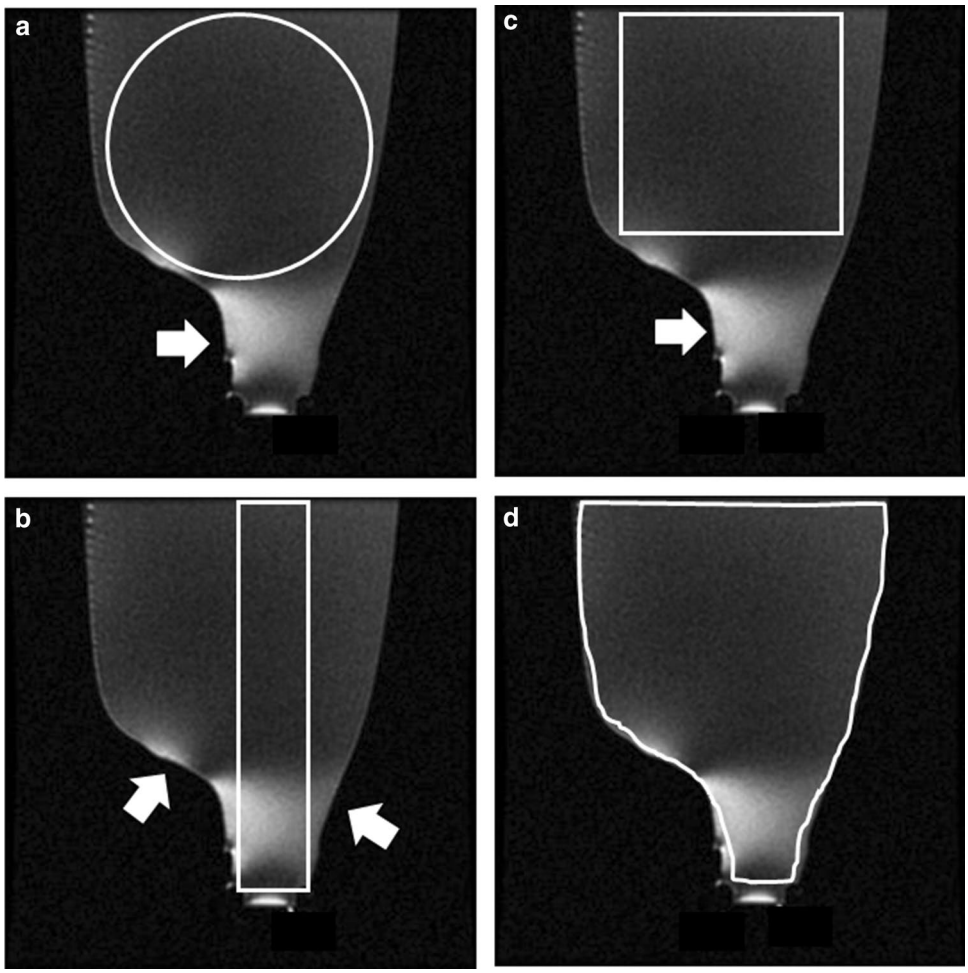

Fig. 1 ROI setting. When using the conventional ROI (square or circle), it may not include the areas with poor uniformity satisfactorily in the peripheral regions (arrow) (**a**–**c**). When they are manually identified, individual differences and human error is considered to be valid concerns (**d**)

poor uniformity in fat suppression, subsequently followed by reporting the volume of high signal intensity regions [5, 7]. However, the volume of these regions may differ depending on the threshold value. If the border between uniform and non-uniform fat suppression regions is unclear, a segmentation error might occur using Laplacian or differential histogram methods because of an incorrect threshold determination.

ROIs can also be manually defined for the whole-body phantom image. During their manual identification, individual differences and human error are considered as valid concerns (Fig. 1d).

Evaluation of the uniformity of fat suppression can be improved using the whole image, to avoid the errors associated with manual ROI selection. If the outline of the phantom was automatically extracted, using the non-fat suppression image, we could then perform the auto segment ROI method, i.e., the "mask method", which is significantly advantageous over the manual ROI method.

Therefore, we developed a "mask method" to evaluate the uniformity of fat suppression using information provided by the whole image, including the areas associated with poor uniformity, to present its effectiveness by acquiring data after using an unevenness phantom and in evaluating ROIs of different sizes.

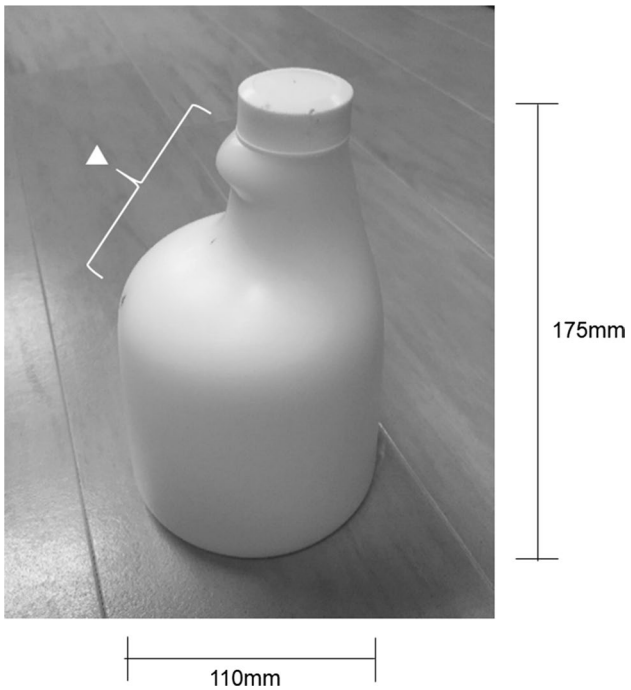

Fig. 2 Appearance of the phantom. Materials that changed the uniformity of fat suppression were placed on the phantom neck well contact (*arrowhead*)

2 Materials and methods

2.1 Ethical consideration

Because this was a phantom study, Institutional Review Board's approval was not required.

2.2 Phantom

We used a combination ratio of 2500 mL of salad oil (as fat), 2500 mL of water, 500 mL of liquid detergent, and 17 g of 100% xanthan gum (Marugo Corporation, Saitama, Japan) in a plastic bottle (1000 mL, 175 mm × 110 mm Φ [height × bottom Φ]). The T1 and T2 relaxation times were 538.04 ms and 49.03 ms, respectively. We acquired images with poor fat suppression using the structure of the bottle neck located between the injection port and the phantom body. The phantom is in Fig. 2. We performed neck study for this phantom study.

To alter the uniformity of fat suppression, the relevant property-altering materials were placed in a polyethylene bag (189 mm × 177 mm), which was then placed on a phantom neck well contact. The following materials (in their respective concentrations) were placed in each bag: rice (1573 g), barium sulfate (98.8%, 1053 g), ball bearings (polystyrene, 364 g), and manganese (II) chloride tetrahydrate (Man) (200 mmol/L) (Fig. 3).

2.3 Imaging conditions

Images were acquired on a 1.5 T MRI scanner equipped with a quadrature head coil (Brivo MR355, GE, Healthcare, Milwaukee, WI, USA).

Assuming the use of the contrast medium, T1-weighted images representing a routine head–neck protocol image were acquired with the following sequence parameters: two-dimensional spin echo (2D SE) [repetition time (TR), 500 ms; echo time (TE), 11 ms; field of view (FOV), 16 × 16 cm; matrix, 160 × 160; slice thickness, 5 mm; number of excitations (NEX), 1; band width (BW), ± 15.63 kHz; flip angle (FA), 80°; number of slice, 1; center frequency (CF), 63,879,190 Hz; and scan time, 1 min 28 s] and three-dimensional fast spoiled gradient echo (3D FSPGR) (TR, 17.7 ms; TE, 2.09 ms; FOV, 16 × 16 cm; matrix, 160 × 160; slice thickness, 2 mm; NEX, 1; BW, ± 15.63 kHz; FA, 20°; number of slice, 15; CF, 63,879,192 Hz; and scan time, 1 min 10 s). The center of the slice was used for the analyses. We used chemical shift selective (CHESS) imaging technique as a method to suppress adipose tissue signals, following which we obtained the sagittal images. To exclude the dependency of the size of volume-shimming, we shimmed the whole slice image. Furthermore, we monitored

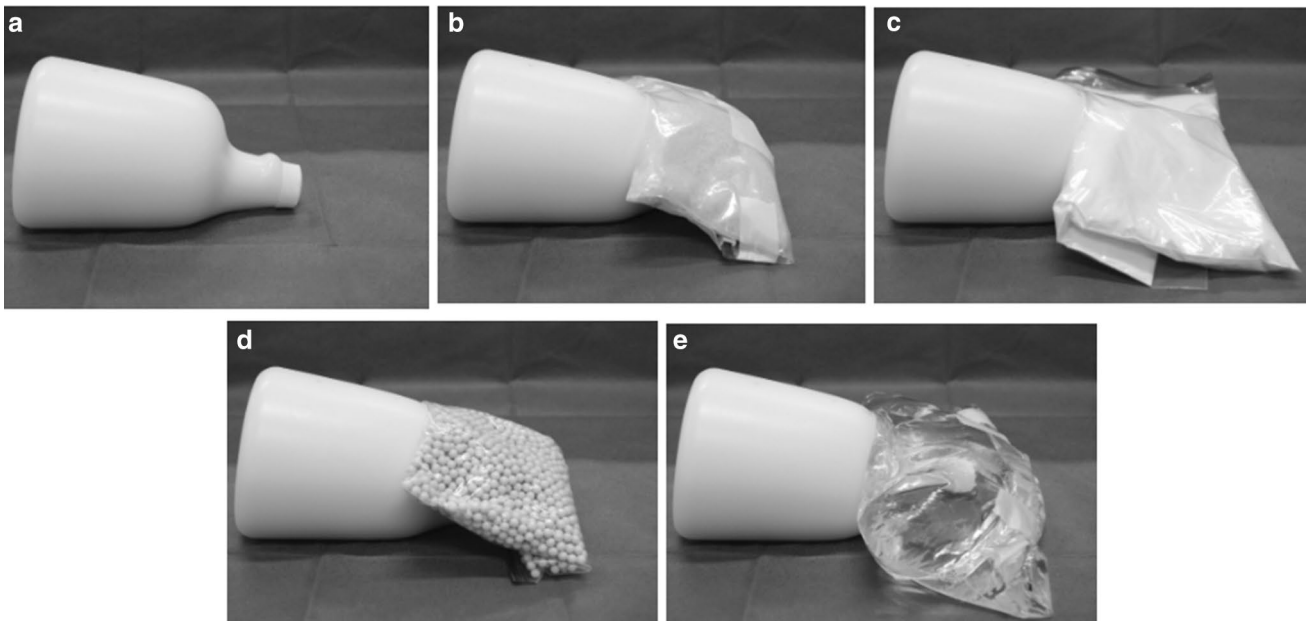

Fig. 3 Method of alteration of the uniformity of fat suppression. The uniformity of fat suppression property-altering materials was placed on the phantom neck. **a** Without materials, **b** rice, **c** barium sulfate, **d** ball bearings, and **e** manganese (II) chloride tetrahydrate

and maintained the receiver gain, and the scan was continuously triplicated. To analyze the image, a non-fat suppression image was obtained using each of the abovementioned sequence parameters, except CHESS. The scan results were acquired thrice, and the data were averaged.

2.4 Image analysis

We generated an image from the non-fat suppression images using discriminant analysis as described by Otsu [11]; it was binarized as a "mask image" and recorded in the form of textual data. The Otsu method is an algorism to automatically decide the threshold depending on the image using binarization.

We then applied the "mask image" to a fat-suppressed image, to effectively remove the background and produce a phantom-only image; this method was called the "mask method" (Fig. 4).

2.5 Image measurement

The largest ROI (100%) is the phantom area obtained using the "mask method". To assess the difference depending on the size of ROI, the ROI contour was consecutively eroded by one pixel until its area reduced from 100% to approximately 50% (49.7%) (Fig. 5) using the uniformity of fat suppression property-altering materials.

NAAD was calculated to evaluate the uniformity of fat suppression.

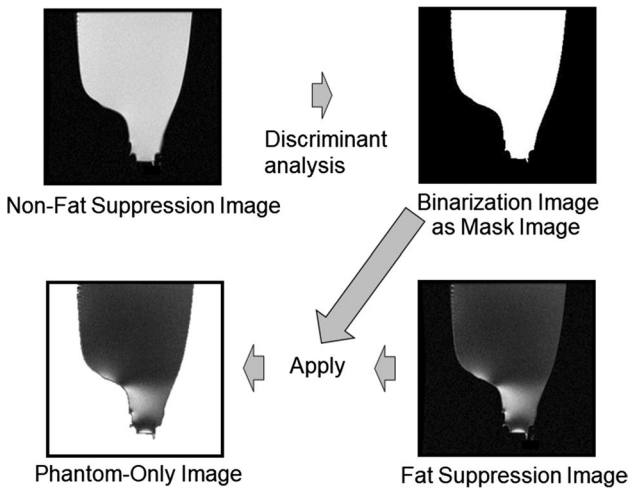

Fig. 4 Diagrammatic representation of the "mask method"

To estimate a free-hand ROI, a boundary just within the contour of the phantom (eroded by one pixel) of a 97.3% ROI was created. It is important to note that while carefully generating the ROI using freehand, it should not be over the contour of the phantom image. Therefore, we assumed that the ROI generated within the phantom image was as large as possible and that the contour (100%) was eroded at a rate of one pixel. The area of the ROI changed from 100 to 97.3% due to the erosion of a single pixel. Moreover, based on NEMA's definition [10], the ROI area should be $\geq$ 75%. Therefore, with the consecutive erosion of the ROI, 76.2% was the closest achieved area of the ROI.

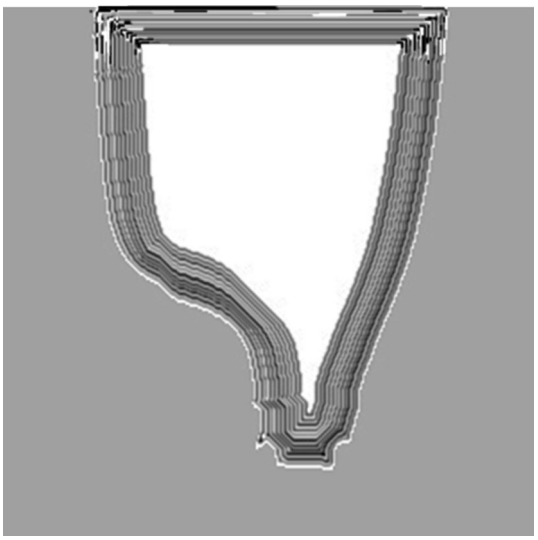

Fig. 5 Eroded for the contour of phantom. Phantom area as the region of interest was reduced from 100 to 49.7% by one pixel

Therefore, we compared the NAAD values of that between 100 and 97.3% and between 100 and 76.2%, in a total of five property-altering materials associated with the uniformity of fat suppression. Wilcoxon paired-rank test was used for statistical analyses. Statistical significance was determined as $P < 0.01$. Moreover, the error was calculated as the difference in NAAD between the areas of 100–49.7% using each uniformity of fat suppression property-altering material.

Error was calculated using the following equation:

$$\text{Error} = \text{NAAD}_i - \text{NAAD}_{100}.$$

Here, NAAD_i is NAAD in ROI size i and NAAD_{100} is NAAD in 100% ROI.

Image analysis and measurement was performed using Image J (v. 1.52a, National Institute of Health, Bethesda, MD, USA) and Microsoft Excel (Microsoft, Redmond, WA, USA) and statistical analyses were performed using EZR (v. 1.37 [12]).

3 Results

Images obtained via 2D SE and 3D FSPGR are presented in Figs. 6 and 7, respectively.

A decrease in the ROI percentage of the phantom was directly correlated to increased NAAD for every MROI below 100%.

Considering 2D SE, NAAD for the data acquired without adding property-altering materials to alter the uniformity of fat suppression was at a steeper percentage, specifically between 67.6 and 49.7% compared to others. The "Man" placed on the phantom neck well contact demonstrated no substantial changes in NAAD between 89.9 and 76.2% (Fig. 8a).

With regard to 3D FSPGR, NAAD for all materials demonstrated a steep inclination between 100 and 92.3% compared to others, and in the absence of property-altering materials associated with the uniformity of fat suppression

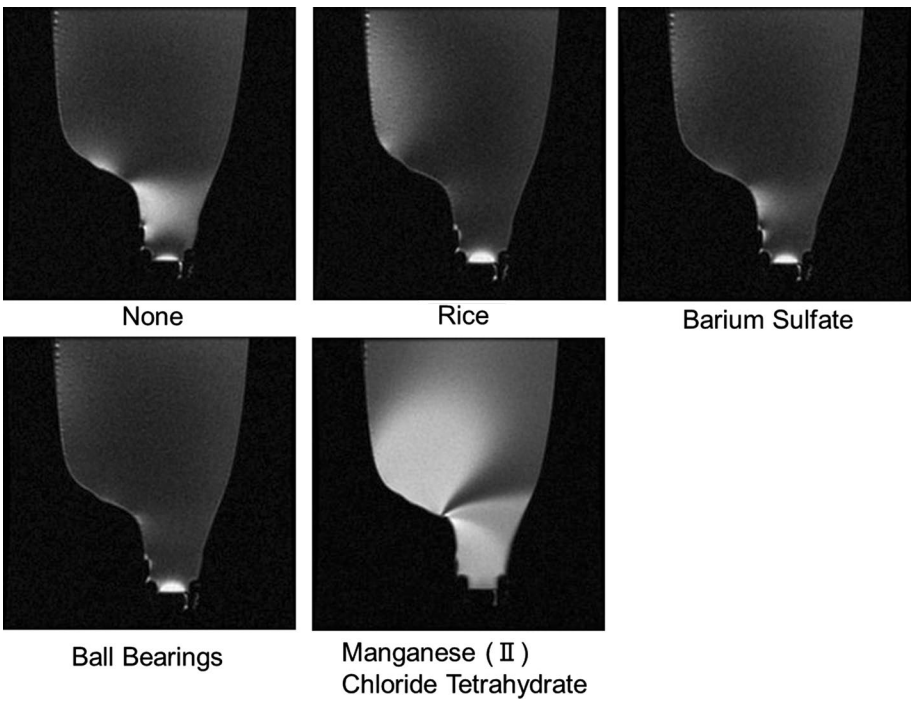

Fig. 6 Images of two-dimensional spin echo. To alter the uniformity of fat suppression, property-altering materials (rice, barium sulfate, ball bearings, and manganese (II) chloride tetrahydrate) were placed on the phantom neck well contact. "None" indicates an absence of material

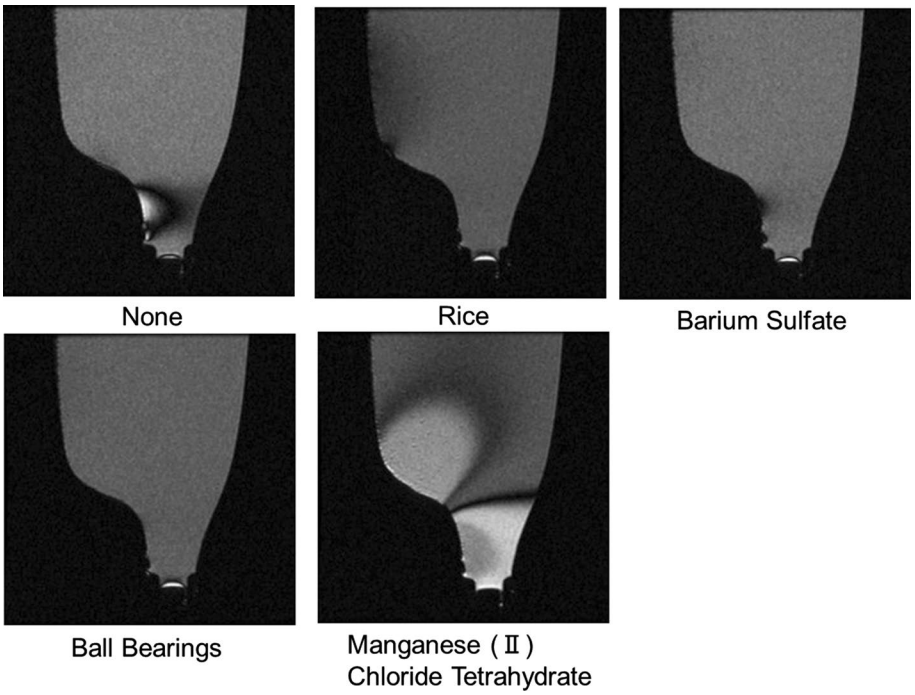

Fig. 7 Images of three-dimensional fast spoiled gradient echo. To alter the uniformity of fat suppression, the property-altering materials (rice, barium sulfate, ball bearings, and manganese (II) chloride tetrahydrate) were placed on the phantom neck well contact. "None" indicates an absence of material

(none) we noted a steep inclination between 65.4 and 49.7% than others. However, the rate of change was smaller than that for 2D SE (Fig. 8b).

Difference between 100 and 97.3%, along with 100 and 76.2% in five samples was described below.

The median (interquartile range) 100, 97.3, and 76.2% area in 2D SE was 70.94 (13.57), 71.75 (13.45), and 74.6 (13.67), respectively (Fig. 9a, b) and their difference was statistically significant ($P < 0.01$). The median (interquartile range) 100, 97.3, and 76.2% area in 3D FSPGR was 87.42 (6.99), 89.52 (6.66), and 92.54 (6.46), respectively (Fig. 9c, d), and their difference was statistically significant ($P < 0.01$).

When the percentage of ROI of the phantom was reduced, we observed an increase in the frequency of errors for every MROI less than 100%.

The error between 67.6 and 49.7% for 2D SE and 65.5 and 49.7% for 3D FSPGR was greater than that for others. 3D FSPGR had a smaller rate of change of error than 2D SE. With regard to 2D SE, ball bearings were found to be the most stable; however, between 100 and 89.9%, they were more steeply inclined than others (Fig. 10).

4 Discussion

We considered that this mask method could be proposed as the feasibility study to measure the uniformity of fat suppression. We could easily and accurately assess the uniformity of fat suppression, by extracting the phantom from the background using the "mask image" method on an image without fat suppression. This may be attributed to the inclusion of the whole are demonstrating poor uniformity area. Consequently, an image of the phantom without the background could be extracted via discriminant analysis because of clear contrast between the phantom and surrounding air. We were concerned that when an area demonstrating poor uniformity in fat suppression was extracted and assessed as a volume data using only an image of fat suppression through binarization, the data could be influenced, depending on the set for the threshold value. Therefore, the "mask method" was more suitable to assess the whole-body phantom image.

With the "mask method", the phantom contour could be objectively and quantitatively determined.

Since, NAAD increased as MROI reduced, fat suppression uniformity was overestimated.

The size of the ROI was set at a minimum 75% of the image of phantom when defined by NEMA. However, NAADs were significantly different between ROI areas of 100% and 76.2% ($P < 0.01$). Therefore, if ROI area was ordered and set, the assessment value would differ.

A 97.3% ROI was selected to represent a free-hand ROI placed just within the wall of the phantom, and there was a significant difference ($P < 0.01$). Considering the free-hand ROI, uniformity of fat suppression was absolutely overestimated compared with the assessment of the whole phantom image. Moreover, due to the subjective nature of the free-hand ROI, the tendency to overestimate the uniformity would be different depending on the evaluator. Therefore, when the percentage of ROI of the phantom was reduced,

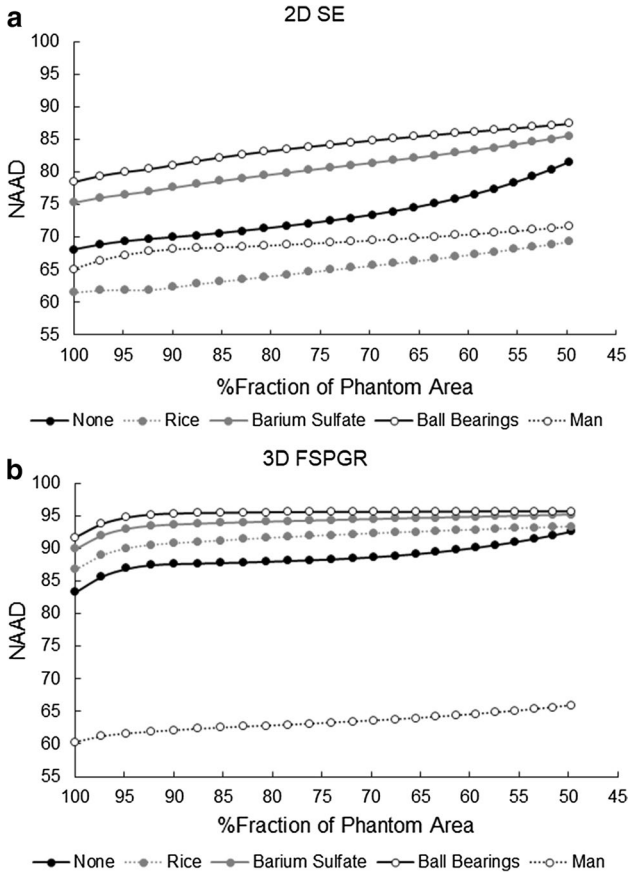

Fig. 8 Results of the measurement of normalized absolute average deviation (NAAD). Two-dimensional spin echo (2D SE) (**a**) and three-dimensional fast spoiled gradient echo (3D FSPGR) (**b**). "None" indicates an absence of material; "Man" indicates manganese (II) chloride tetrahydrate

NAAD increased because the area with poor uniformity was not satisfactorily included in the ROI in the peripheral regions.

The "mask method" approach has high reproducibility as long as the phantom image is extracted using a constant algorithm. Therefore, if the algorithm is reliable, measurements of the uniformity of fat suppression will be highly accurate.

When the percentage of an area of the ROI decreased, NAAD and error increased for every image. We considered that because that poor fat suppression area in vicinity of bottle neck was influenced. This tendency was strongly reflected. Especially, "None" had a tendency of increasing error when the ROI was reduced due to the area of the uniformity of poor fat suppression, which was included in ROI, differed depending on the size of the ROI.

In Fig. 6, a large poor-fat-suppression area is observed in "Man". visually; however, the result of NAAD was higher than that of "Rice" (Fig. 8a) primarily because the high signal area was excessively wide and uniform. NAAD was calculated by the individual pixel value and the absolute deviation. We considered that dispersion of the data was higher in "Rice" than in "Man". Therefore, when the poor fat suppression area was uniform, wide and excessively, NAAD might be increased. If you use the NEMA method, the same phenomenon might occur. In such situations, the calculation for the uniformity and visual assessment might be separated. Actually, in Fig. 6, we considered that dispersion of the data was lower in "Rice" than in "Man"; therefore, "Rice" of NAAD was higher than "Man" of NAAD (Fig. 8a).

As shown in Fig. 7a, NAAD of "Man" remained unchanged between 90 and 76% for 2D SE possibly

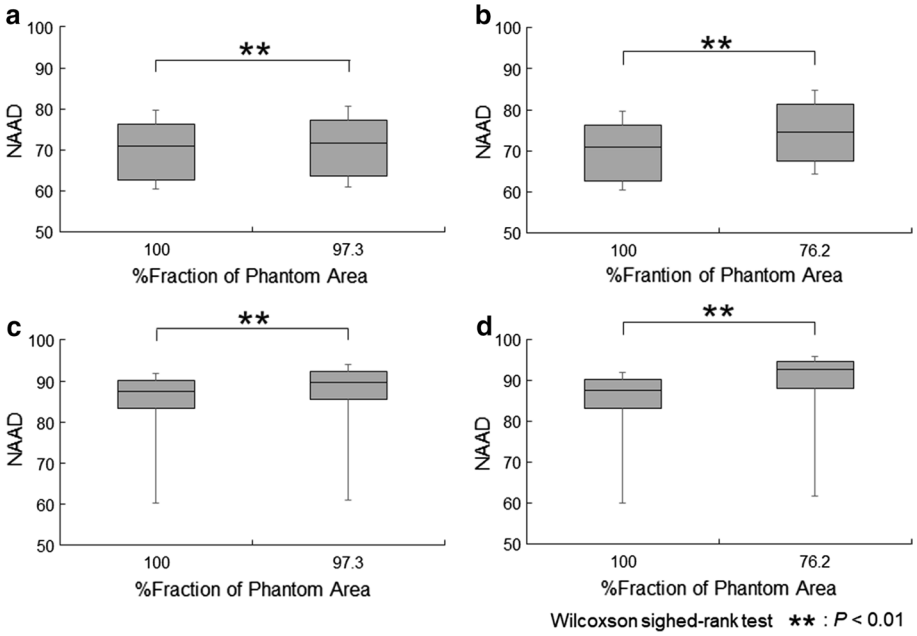

Fig. 9 Percent fraction of phantom area based on NAAD. Between 100 and 97.3% (**a**) and between 100 and 76.2% for two-dimensional spin echo (**b**) and between 100 and 97.3% (**c**) and between 100 and 76.2% (**d**) for three-dimensional fast spoiled gradient echo

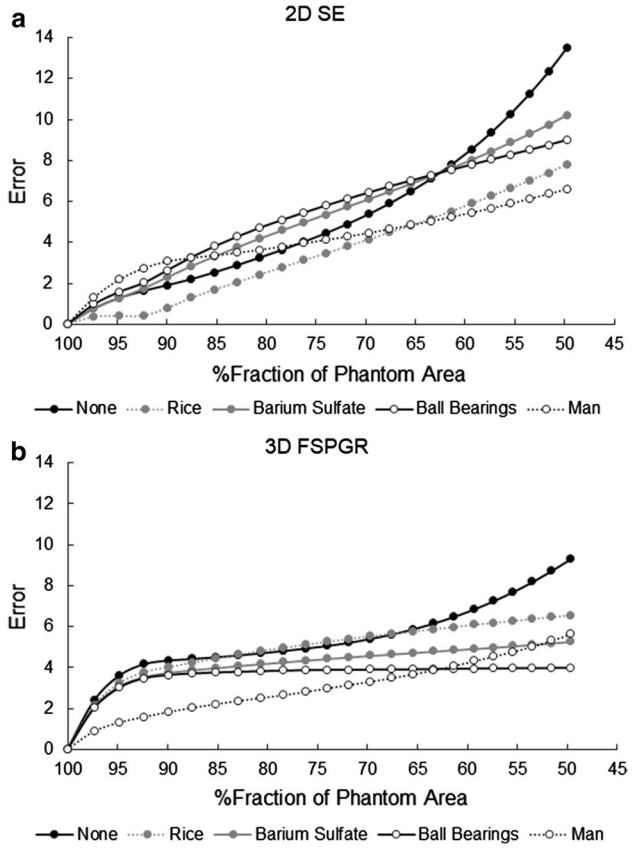

Fig. 10 Results of the measurement of error. Two-dimensional spin echo (2D SE) (**a**) and three-dimensional fast spoiled gradient echo (3D FSPGR) (**b**). "None" indicates an absence of material; "Man" indicates manganese (II) chloride tetrahydrate

because of the expansion of poor fat suppression from the center to the peripheral area of the phantom. Alternatively, for an area with steep inclination, NAAD and error changed depending on the size of the ROI mainly since we considered that there was a reduction in the rate of the poor uniformity of fat suppression.

Unlike PIU, which is sensitive to the SNR of an image, NAAD is a suitable method for the assessment of uniformity of fat suppression because it was calculated by absolute average deviation and not overestimated for noise.

The "mask method" is not limited to the size and shape of the object being imaged. Whole phantom data could be obtained compared with using many ROIs of the smallest possible size including the periphery. Moreover, the "mask method" has a high reliability due to the absence of human error and individual dependency and because of its accuracy compared with manual selection.

There are several limitations to the study that need to be addressed. In this study, we assumed that this "mask method" could be performed using any software; however, the use of another software (e.g., MATLAB MathWorks, Inc., Massachusetts, USA) may improve work efficiency.

The use of a phantom is an ideal scenario for quantitative assessment during an objective physical evaluation; however, selection of the right shape might be difficult. Herein, the phantom was created based on actual clinical data [5, 7], but reproducing its anatomy is difficult. Moreover, including a phantom in a clinical study might not be feasible. However, we considered that fat suppression tendency index could be assessed when sequence parameter or scan method was changed.

We only used NAAD to assess areas demonstrating poor uniformity in fat suppression and did not compare it with other methods. However, although any uniformity assessment was used, whole phantom area could be assessed only to use the "mask method".

When many ROIs are used, results may alter depending on the size of these ROIs. In actuality, obtaining the whole phantom data is difficult if many ROIs are used.

Furthermore, if the position or field of view of an image changes between with and without fat suppression acquisitions, the "mask method" cannot be applied due to misregistration of the mask image on the fat suppression image.

Moreover, the influence of chemical shift was not evaluated. We were concerned that a strong chemical shift would be an issue for the image acquired without fat suppression; however, the chemical shift was not remarkable and did not influence the phantom-related calculations in this study.

We did not attempt to implement other fat suppression methods (e.g., Dixon method); however, the frequency-selective fat suppression method was generally used.

We assumed when diffusion-weighted image with echo-planner imaging was used, that distortion could be influenced due to motion-probing gradient.

The "mask method" may be difficult to use in clinical imaging, due to heterogeneous contents, including any tissues, and two images should be obtained, with and without fat suppression. However, this method could be used for phantoms based on a clear contour and uniform contents.

When a clinical image is assessed, manual extraction of fat ROIs [13] could be suitable. However, when objective and quantitative assessment is performed, a phantom study could be useful.

Furthermore, we believe that the "mask method" could be used for assessing B1 uniformity, and that this method has great potential as a new assessment method in future studies.

In the present study, the "mask method" was used to evaluate the uniformity of fat suppression wherein we noted poor uniformity attributed to poor B1 or B0 uniformity in peripheral regions. General uniformity could be assessed while including the peripheral regions using the "mask method"; however, this has not been previously performed. The general uniformity was not evaluated in this study; therefore,

there was no guarantee of the results. Furthermore, according to the NEMA standard, the ROI covering at least 75% of the phantom image must exclude peripheral regions. Therefore, currently herein, we considered the "mask method" for assessing uniformity of fat suppression.

We considered that when uniformity of fat suppression was assessed, e.g., for volume-shimming dependency [5] or sequence dependency [7], to improve its uniformity, more objective, concrete, and accurate data could be obtained by the "mask method" provided that the whole phantom is included in the assessment.

5 Conclusion

We developed a mask method to evaluate the uniformity of fat suppression using whole phantom image, including the whole poor uniformity area, and assessed its usefulness by performing calculation depending on the size of an ROI.

Funding This research received no specific grant from any funding agency in the public, commercial, or not-for-profit sectors.

Compliance with ethical standards

Ethical approval This article does not contain any studies with human participants or animals performed by any of the authors.

Conflict of interest All authors declare that there is no conflict of interest.

References

1. Bernstein MA, King KF, Zhou XJ. Chapter 4, spectral radiofrequency pulses. In: Bernstein MA, King KF, Zhou XJ, editors. Handbook of MRI pulse sequences. London: Elsevier Academic; 2004. p. 96–124.
2. Bernstein MA, King KF, Zhou XJ. Chapter 5, spatial radiofrequency pulses. In: Bernstein MA, King KF, Zhou XJ, editors. Handbook of MRI pulse sequences. London: Elsevier Academic; 2004. p. 125–76.
3. Bernstein MA, King KF, Zhou XJ. Chapter 6, adiabatic radiofrequency pulses. In: Zhou XJ, editor. Handbook of MRI pulse sequences. London: Elsevier Academic; 2004. p. 177–214.
4. Reeder SB, Yu H, Johnson JW, Shimakawa A, Brittain JH, Pelc NJ, Beaulieu CF, Gold GE. T1- and T2-weighted fast spin-echo imaging of the brachial plexus and cervical spine with IDEAL water-fat separation. J Magn Reson Imaging. 2006;24:825–32.
5. Takatsu Y, Nishiyama K, Miyati T, Miyano H, Kajihara M, Akasaka T. A comparison of shimming techniques for optimizing fat suppression in MR mammography. Radiol Phys Technol. 2013;6:486–91.
6. Rosen Y, Bloch BN, Lenkinski RE, Greenman RL, Marquis RP, Rofsky NM. 3T MR of the prostate: reducing susceptibility gradients by inflating the endorectal coil with a barium sulfate suspension. Magn Reson Med. 2007;57:898–904.
7. Takatsu Y, Kyotani K, Ueyama T, Miyati T, Yamamura K, Andou A. Assessment of the quality of breast MR imaging using the modified Dixon method and frequency-selective fat suppression: a phantom study. Magn Reson Med Sci. 2018;17:350–5.
8. Mirowitz SA, Apicella P, Reinus WR, Hammerman AM. MR imaging of bone marrow lesions: relative conspicuousness on T1-weighted, fat-suppressed T2-weighted, and STIR images. Am J Roentgenol. 1994;162:215–21.
9. Le-Petross H, Kundra V, Szklaruk J, Wei W, Hortobagyi GN, Ma J. Fast three-dimensional dual echo dixon technique improves fat suppression in breast MRI. J Magn Reson Imaging. 2010;31:889–94.
10. National Electrical Manufacturers Association, Determination of image uniformity in diagnostic magnetic resonance images. NEMA Standards Publication MS 3-2008 (NEMA, Rosslyn, VA, 2008), 2008. pp. 1–17.
11. Otsu N. A threshold selection method from gray-level histograms. IEEE Trans Syst Man Cybern. 1979;9(1):62–6.
12. Kanda Y. Investigation of the freely available easy-to-use software'EZR' for medical statistics. Bone Marrow Transpl. 2013;48:452–8.
13. Takatsu Y, Akasaka T, Miyati T. The Dixon technique and the frequency-selective fat suppression technique in three-dimensional T1 weighted MRI of the liver: a comparison of contrast-to-noise ratios of hepatocellular carcinomas-to-liver. Br J Radiol. 2015;88:20150117.